WATER RESOURCES RESEARCH, VOL. 34, NO. 1, PAGES 21–32, JANUARY 1998

Transient effective hydraulic conductivities under slowly and rapidly varying mean gradients in bounded three-dimensional random media

Daniel M. Tartakovsky[1] and Shlomo P. Neuman

Department of Hydrology and Water Resources, The University of Arizona, Tucson

Abstract. We have shown elsewhere [*Tartakovsky and Neuman*, this issue (a)] that in randomly heterogeneous media, the ensemble mean transient flux is generally nonlocal in space-time and therefore non-Darcian. We have also shown [*Tartakovsky and Neuman*, this issue (b)] that there are special situations in which this flux can be localized so as to render it Darcian in real or transformed domains. Each such situation gives rise to an effective hydraulic conductivity which relates mean gradient to mean flux at any point in real or transformed space-time. In this paper we develop first-order analytical expressions for effective hydraulic conductivity under three-dimensional transient flow through a box-shaped domain due to a mean hydraulic gradient that varies slowly in space and time. When the mean gradient varies rapidly in time, the Laplace transform of the mean flux is local but its real-time equivalent includes a temporal convolution integral; we develop analytical expressions for the real-time kernel of this convolution integral. The box is embedded within a statistically homogeneous natural log hydraulic conductivity field that is Gaussian and exhibits an anisotropic exponential spatial correlation structure. By the effective hydraulic conductivity of a finite box in such a field we imply the ensemble mean (expected value) of all random equivalent conductivities that one could associate with the box under these conditions. We explore the influence of domain size, time, and statistical anisotropy on effective conductivity and include a simple new formula for its variation with statistical anisotropy ratio in an infinite domain under steady state.

1. Introduction

Consider Darcy's law and the transient continuity equation

$$\mathbf{q}(\mathbf{x}, t) = -K(\mathbf{x})\nabla h(\mathbf{x}, t)$$
$$S\,\frac{\partial h(\mathbf{x}, t)}{\partial t} = -\nabla\cdot\mathbf{q}(\mathbf{x}, t) \qquad \mathbf{x}\in\Omega \tag{1}$$

subject to initial and boundary conditions

$$h(\mathbf{x}, 0) = H_0(\mathbf{x}) \qquad \mathbf{x}\in\Omega \tag{2}$$

$$h(\mathbf{x}, t) = H(\mathbf{x}, t) \qquad \mathbf{x}\in\Gamma_D \tag{3}$$

$$-\mathbf{q}(\mathbf{x}, t)\cdot\mathbf{n}(\mathbf{x}) = 0 \qquad \mathbf{x}\in\Gamma_N. \tag{4}$$

Here Ω is the flow domain, $\mathbf{q}$ is flux, K is a random hydraulic conductivity field, h is hydraulic head, S is known specific storage, H_0 is a random initial head distribution, H is random head on Dirichlet boundary segments Γ_D, Γ_N are mean no-flow Neumann boundary segments, and $\mathbf{n}$ is a unit outward normal to the boundary Γ, which in turn forms the union of Γ_D and Γ_N. The functions H_0 and H are prescribed in statistically independent manners. All quantities are defined on a local support scale $\omega \ll \Omega$.

Let the natural log hydraulic conductivity $Y(\mathbf{x}) = \ln K(\mathbf{x})$ form a statistically homogeneous field with constant mean (expectation) $\langle Y(\mathbf{x})\rangle$ and variance σ_Y^2. We consider the special case where $\sigma_Y^2 < 1$. It has been shown by *Tartakovsky and Neuman* [this issue (a)] that then, to second-order in σ_Y (first-order in σ_Y^2),

$$\langle\mathbf{q}^{[2]}(\mathbf{x}, t)\rangle = \mathbf{q}^{(0)}(\mathbf{x}, t) + \langle\mathbf{q}^{(2)}(\mathbf{x}, t)\rangle \tag{5}$$

where

$$\mathbf{q}^{(0)}(\mathbf{x}, t) = -K_G\nabla h^{(0)}(\mathbf{x}, t) \tag{6}$$

and

$$\langle\mathbf{q}^{(2)}(\mathbf{x}, t)\rangle = -K_G\left[\nabla\langle h^{(2)}(\mathbf{x}, t)\rangle + \frac{\sigma_Y^2}{2}\nabla h^{(0)}(\mathbf{x}, t)\right] + \mathbf{r}^{[2]}(\mathbf{x}, t). \tag{7}$$

Here [2] denotes the sum of all terms containing σ_Y raised up to second power, (n) denotes terms that contain only nth powers of σ_Y, and $K_G = \exp\langle Y\rangle$ is the geometric mean of $Y(\mathbf{x})$. The zeroth-order mean head $h^{(0)}(\mathbf{x}, t)$ satisfies (1)–(4) with $K(\mathbf{x})$ replaced by K_G and with $H_0(\mathbf{x})$, $H(\mathbf{x}, t)$ replaced by their ensemble means, $\langle H_0(\mathbf{x})\rangle$, $\langle H(\mathbf{x}, t)\rangle$, respectively. The second-order mean head correction $\langle h^{(2)}(\mathbf{x}, t)\rangle$ satisfies

$$S(\mathbf{x})\,\frac{\partial\langle h^{(2)}(\mathbf{x}, t)\rangle}{\partial t} = -\nabla\cdot\langle\mathbf{q}^{(2)}(\mathbf{x}, t)\rangle \tag{8}$$

subject to homogeneous mean initial and boundary conditions. The "residual flux" $\mathbf{r}(\mathbf{x}, t)$ is given to second order by

$$\mathbf{r}^{[2]}(\mathbf{x}, t) = \int_0^t\int_\Omega \mathbf{a}^{[2]}(\mathbf{y}, \mathbf{x}, t-\tau)\nabla_y h^{(0)}(\mathbf{y}, \tau)\,d\mathbf{y}\,d\tau \tag{9}$$

[1]Now at Geoanalysis Group, Earth and Environmental Sciences Division, Los Alamos National Laboratory, Los Alamos, New Mexico.

Paper number 97WR01965.
0043-1397/98/97WR-01965$09.00

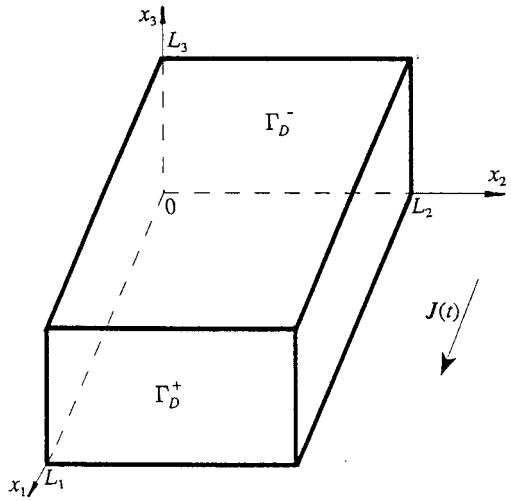

Figure 1. Box-shaped flow domain Ω with Dirichlet and Neumann boundaries.

where

$$\mathbf{a}^{[2]}(\mathbf{y}, \mathbf{x}, t-\tau) = K_G^2 C_Y(\mathbf{y}, \mathbf{x}) \nabla_x \nabla_y^T G^{(0)}(\mathbf{y}, \mathbf{x}, t-\tau), \quad (10)$$

$C_Y(\mathbf{y}, \mathbf{x}) = \langle Y'(\mathbf{y})\, Y'(\mathbf{x}) \rangle$ is the spatial autocovariance of Y, and $G^{(0)}$ is a zeroth-order Green's function. The Green's function $G^{(0)}(\mathbf{y}, \mathbf{x}, t-\tau)$ is obtained in the same manner as $h^{(0)}$ but with a Dirac delta source $\delta(\mathbf{x}-\mathbf{y})\delta(t-\tau)$ subject to zero initial and boundary conditions.

In this paper we develop analytical expressions for unconditional effective hydraulic conductivity under three-dimensional transient flow through a box-shaped domain due to a mean hydraulic gradient $\mathbf{J}(t)$ that is spatially uniform but varies either slowly or rapidly in time. The box is embedded within a statistically homogeneous natural log hydraulic conductivity field Y that is Gaussian and exhibits an anisotropic exponential autocorrelation structure. Then $\langle h^{(2)}(\mathbf{x}, t) \rangle \equiv 0$ and, when $\mathbf{J}(t)$ varies slowly in time (has a negligibly small time derivative), one can approximate (9) by the local expressions [*Tartakovsky and Neuman*, this issue (b)]

$$\mathbf{r}^{[2]}(\mathbf{x}, t) \approx \boldsymbol{\kappa}^{[2]}(\mathbf{x}, t)\mathbf{J}(t) \quad (11)$$

$$\langle \mathbf{q}^{[2]}(\mathbf{x}, t) \rangle \approx -\mathbf{K}_{eff}^{[2]}(\mathbf{x}, t)\mathbf{J}(t). \quad (12)$$

Here

$$\boldsymbol{\kappa}^{[2]}(\mathbf{x}, t) = K_G^2 \int_0^t \int_\Omega C_Y(\mathbf{y}, \mathbf{x}) \nabla_x \nabla_y^T G^{(0)}(\mathbf{y}, \mathbf{x}, t-\tau)\, d\mathbf{y}\, d\tau \quad (13)$$

is a symmetric positive-semidefinite tensor (dyadic) and

$$\mathbf{K}_{eff}^{[2]}(\mathbf{x}, t) = K_G \left[1 + \frac{\sigma_Y^2}{2} \right] \mathbf{I} - \boldsymbol{\kappa}^{[2]}(\mathbf{x}, t) \quad (14)$$

is a symmetric positive-definite dyadic, $\mathbf{I}$ being the identity matrix. Note that quantities other than $\mathbf{J}(t)$ in (11) and (12) may remain dependent on $\mathbf{x}$ because of boundary effects.

Tartakovsky and Neuman [this issue (b)] have shown that when a uniform mean gradient varies rapidly with time, taking the Laplace transform of (9) yields the local expressions

$$\tilde{\mathbf{r}}^{[2]}(\mathbf{x}, \lambda) = \bar{\boldsymbol{\kappa}}^{[2]}(\mathbf{x}, \lambda)\tilde{\mathbf{J}}(\lambda) \quad (15)$$

$$\langle \tilde{\mathbf{q}}^{[2]}(\mathbf{x}, \lambda) \rangle = -\bar{\mathbf{K}}_{eff}^{[2]}(\mathbf{x}, \lambda)\tilde{\mathbf{J}}(\lambda) \quad (16)$$

where the tilde denotes the Laplace transform, λ is the corresponding transform parameter, and

$$\bar{\boldsymbol{\kappa}}^{[2]}(\mathbf{x}, \lambda) = K_G^2 \int_\Omega \mathbf{C}(\mathbf{y}, \mathbf{x}) \nabla_x \nabla_y^T \tilde{G}^{(0)}(\mathbf{y}, \mathbf{x}, \lambda)\, d\mathbf{y} \quad (17)$$

$$\bar{\mathbf{K}}_{eff}^{[2]}(\mathbf{x}, \lambda) = K_G \left[1 + \frac{\sigma_Y^2}{2} \right] \mathbf{I} - \bar{\boldsymbol{\kappa}}^{[2]}(\mathbf{x}, \lambda). \quad (18)$$

The latter is a symmetric positive-definite dyadic which constitutes an effective hydraulic conductivity tensor in Laplace space.

The inverse Laplace transform of (16), considering (17) and (18), is

$$\langle \mathbf{q}^{[2]}(\mathbf{x}, t) \rangle = -K_G \left[1 + \frac{\sigma_Y^2}{2} \right] \mathbf{J}(t) + \int_0^t \boldsymbol{\kappa}^{*[2]}(\mathbf{x}, t-\tau)\mathbf{J}(\tau)\, d\tau \quad (19)$$

where

$$\boldsymbol{\kappa}^{*[2]}(\mathbf{x}, t) = K_G^2 \int_\Omega C_Y(\mathbf{y}-\mathbf{x}) \nabla_x \nabla_y^T G^{(0)}(\mathbf{y}, \mathbf{x}, t-\tau)\, d\mathbf{y} \quad (20)$$

is the inverse Laplace transform of (17).

The remainder of this paper is devoted to analytical evaluation, and subsequent exploration, of the effective parameters in (11), (12), and (19). We start by considering flow through a box of mildly heterogeneous porous media when mean uniform flow varies slowly in space-time and then extend this to account for arbitrary time variation.

2. Slow Time Variation

2.1. Uniform Flow in a Box

Let the superscript p denote Cartesian coordinates oriented parallel to the principal directions of anisotropy associated with the exponential log hydraulic conductivity spatial covariance function

$$C_Y(\mathbf{z}^p) = \sigma_Y^2 \exp\left[-\left(\sum_{i=1}^3 (z_i^p/\lambda_i)^2 \right)^{1/2} \right] \qquad z_i^p = y_i^p - x_i^p \quad (21)$$

where λ_i $(i = 1, 2, 3)$ are principal integral scales and $\mathbf{z}^p$ is a displacement vector. We consider a box with lateral mean no-flow boundaries separated by finite distances equal to L_2 and L_3 and two constant head boundaries a distance L_1 apart (Figure 1). The boundaries of the box are parallel to the principal coordinates. A spatially uniform mean hydraulic gradient $\mathbf{J}(t)$ of magnitude $J_1(t)$ acts between the Dirichlet boundaries parallel to x_1^p. Then $\boldsymbol{\kappa}^{[2]}(\mathbf{x}, t)$ in (13) becomes a directional scalar given by

$$\kappa_1^{[2]}(\mathbf{x}^p, t) = K_G^2 \int_0^t \int_\Omega C_Y(\mathbf{y}^p - \mathbf{x}^p) \frac{\partial^2 G^{(0)}(\mathbf{y}^p, \mathbf{x}^p, t-\tau)}{\partial x_1^p \partial y_1^p}\, d\mathbf{y}^p\, d\tau. \quad (22)$$

By the same token, the mean flux has only one nonzero component

$$\langle q_1^{[2]}(\mathbf{x}^p, t) \rangle \approx -K_{eff,1}^{[2]}(\mathbf{x}^p, t) J_1(t) \quad (23)$$

where

$$K^{[2]}_{eff,1}(\mathbf{x}^p, t) = K_G\left[1 + \frac{\sigma_Y^2}{2}\right] - \kappa_1^{[2]}(\mathbf{x}^p, t). \tag{24}$$

The Green's function $G_s = SG^{(0)}$ for the box satisfies

$$\frac{\partial G_S(\mathbf{y}^p, \mathbf{x}^p, t-\tau)}{\partial \tau} + \lambda_0 \nabla_{y^p} G_S(\mathbf{y}^p, \mathbf{x}^p, t-\tau)$$
$$= -\delta(\mathbf{y}^p - \mathbf{x}^p)\delta(t-\tau) \tag{25}$$
$$\lambda_0 = K_G/S \quad 0 < y_1^p < L_1 \quad 0 < y_2^p < L_2 \quad 0 < y_3^p < L_3,$$

subject to homogeneous initial and boundary conditions

$$G_S(\mathbf{y}^p;\ \mathbf{x}^p;\ 0) = 0$$
$$G_S(0, y_2^p, y_3^p;\ \mathbf{x}^p;\ \eta) = G_S(L_1, y_2^p, y_3^p;\ \mathbf{x}^p;\ \eta) = 0$$
$$\frac{\partial G_S}{\partial y_2^p}(y_1^p, 0, y_3^p;\ \mathbf{x}^p;\ \eta) = \frac{\partial G_S}{\partial y_2^p}(y_1^p, L_2, y_3^p;\ \mathbf{x}^p;\ \eta) = 0 \tag{26}$$
$$\frac{\partial G_S}{\partial y_3^p}(y_1^p, y_2^p, 0;\ \mathbf{x}^p;\ \eta) = \frac{\partial G_S}{\partial y_3^p}(y_1^p, y_2^p, L_3;\ \mathbf{x}^p;\ \eta) = 0$$

where $\eta = t - \tau$. The solution to the boundary value problem (25) and (26) is the product of three one-dimensional solutions [*Carslaw and Jaeger*, 1967, p. 361]. These are given for Dirichlet boundaries by Carslaw and Jaeger's equation 2 (p. 362) and for no-flow boundaries by their equation 7 (p. 361). The corresponding triple product is

$$G_S(\mathbf{y}^p, \mathbf{x}^p, \eta)$$
$$= \frac{2}{L_1 L_2 L_3}\sum_{m=1}^{\infty} e^{-\lambda_0 \pi^2 \eta m^2/L_1^2} \sin\frac{\pi m x_1^p}{L_1} \sin\frac{\pi m y_1^p}{L_1}$$
$$\cdot\left[1 + 2\sum_{n=1}^{\infty} e^{-\lambda_0 \pi^2 \eta n^2/L_2^2} \cos\frac{\pi n x_2^p}{L_2} \cos\frac{\pi n y_2^p}{L_2}\right]$$
$$\cdot\left[1 + 2\sum_{j=1}^{\infty} e^{-\lambda_0 \pi^2 \eta j^2/L_3^2} \cos\frac{\pi j x_3^p}{L_3} \cos\frac{\pi j y_3^p}{L_3}\right]. \tag{27}$$

In terms of normalized length variables $x_i = x_i^p/\lambda_i$, $y_i = y_i^p/\lambda_i$, $z_i = z_i^p/\lambda_i$, $i = 1, 2, 3$, C_Y in (21) takes the isotropic form

$$C_Y(z) = \sigma_Y^2 e^{-z} \qquad z = |\mathbf{z}| = |\mathbf{y} - \mathbf{x}|. \tag{28}$$

Substituting (28) and (27) into (22) and (24), then introducing the dimensionless variables $t_D = K_G t/S\lambda_1^2$, $l_i = L_i/\lambda_i$, $\chi_i = x_i/l_i$, $\zeta_i = y_i/l_i$, $\rho_i = \varepsilon_i l_i$, $\varepsilon_i = \lambda_i/\lambda_1$, $i = 1, 2, 3$, leads to

$$K_{eff,1}(\chi, t_D) = K_G\left[1 + \frac{\sigma_Y^2}{2}\right] - \kappa_1^{[2]}(\chi, t_D)$$
$$\kappa_1^{[2]}(\chi, t_D) = \sigma_Y^2 K_G[D_{st}(\chi) - b(\chi, t_D)] \tag{29}$$

where $\kappa_1^{[2]}$ is given by (A1), D_{st} is given by (A3), and b is given by (A4) in Appendix A. An alternative form for $\kappa_1^{[2]}$ is given by (A2). The alternative form was found by *Paleologos et al.* [1996] to converge faster than (A1) for all but extremely small distances between the Dirichlet boundaries, and it is therefore (A2) that we evaluate numerically by Gaussian quadrature below. Note that $K_{eff,1}$ depends on position in three-dimensional space and time. As will become clear in the subsequent asymptotic analysis, D_{st} represents the steady state component of $K_{eff,1}$, and b represents its transient component.

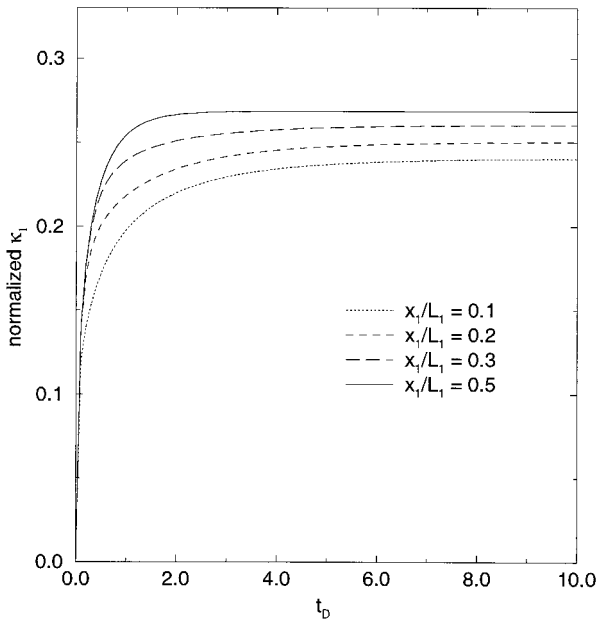

Figure 2. Spatial variation of normalized $\kappa_1^{[2]}$ in box with $\rho_1 = 5$ and $\rho_2 = \rho_3 = 100$.

We start by examining the effect of location within the box on effective hydraulic conductivity. To illustrate this effect we consider a box of dimensions $\rho_1 = 5$ and $\rho_2 = \rho_3 = 100$. Figure 2 shows how $\kappa_1^{[2]}(\chi, t_D)$, normalized by $\sigma_Y^2 K_G$, varies with dimensionless time t_D at various dimensionless distances $\chi_1 = x_1/l_1$ from the Dirichlet boundaries, sufficiently far from the lateral no-flow boundaries, so that these have no effect. It is clearly seen that $\kappa_1^{[2]}(\chi, t_D)$ is affected by distance from the Dirichlet boundaries. Although mass balance requires that this effect vanish asymptotically as time goes to infinity, Figure 2 demonstrates that the effect may nevertheless persist for long time.

Theoretically, as the box shrinks to a point, that is, $\rho_i \to 0$ for all $i = 1, 2, 3$, $\kappa_1^{[2]}(\chi, t_D) \to 0$ because the Green's function (28) vanishes in this limit. It follows from the first equation in (29) that $K_{eff,1} = K_A$. As $\rho_i \to \infty$ for all i, $\kappa_1^{[2]}(\chi, t_D)$ reduces to its infinite domain counterpart originally developed by *Dagan* [1982, equation (45)]. It also follows from (A1) that when $t_D \to 0$, then $\kappa_1^{[2]}(\chi, t_D) \to 0$ and so $K_{eff,1} = K_A$. Since the time integral of the transient Green's function tends asymptotically to the corresponding steady state Green's function as $t_D \to \infty$, $b(\chi, t_D) \to 0$ and thus $\kappa_1^{[2]}(\chi, t_D) \to \sigma_Y^2 K_G D_{st}(\chi)$.

To explore the effect of box size on $\kappa_1^{[2]}(\chi, t_D)$, we evaluate (A2) at the center of the box where $\chi = 0.5$ for several values of $2\rho = \rho_1 = \rho_2 = \rho_3$. The results are shown in Figure 3. They clearly show that as we expect on theoretical grounds, $\kappa_1^{[2]}(t_D)$ diminishes as 2ρ becomes small. The steady state asymptote of $\kappa_1^{[2]}(t_D)$ is virtually equal to its infinite domain theoretical value of 1/3 [*Dagan*, 1982, equation (45)] when $2\rho \geq 7$. One further sees that the relaxation time t_r, required for transient effects to dissipate, increases with 2ρ.

To analyze the behavior of D_{st} as a function of dimensionless cube size 2ρ, we evaluate (A2) for sufficiently large t_D. The

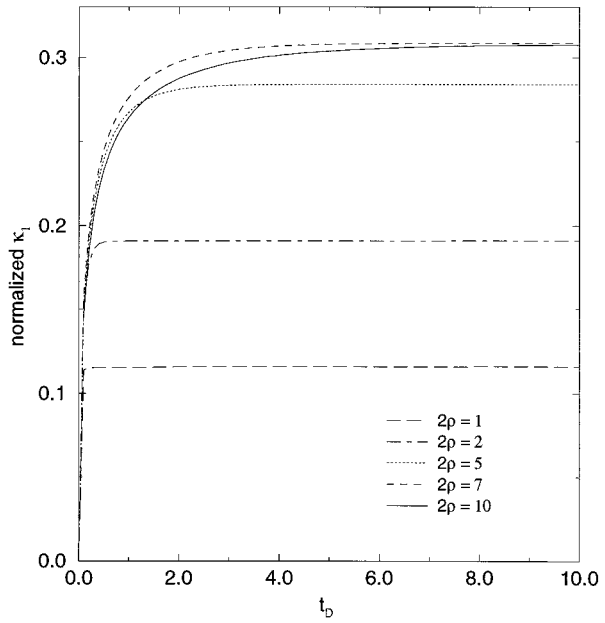

Figure 3. Normalized $\kappa_1^{[2]}$ versus dimensionless time t_D for various dimensionless box sizes $2\rho = \rho_1 = \rho_2 = \rho_3$.

result is shown in Figure 4. We see that D_{st} increases rapidly with 2ρ when the latter is small but then tends very slowly to its asymptotic value of 1/3.

It is important to remember that $\rho_i = \varepsilon_i l_i$ so that the above results represent not only an equidimensional box (cube) in a statistically isotropic Y field but also brick-shaped boxes in anisotropic fields. Varying 2ρ in Figures 3 and 4 thus corresponds either to varying box size when integral scales are fixed (but not necessarily equal), or varying integral scales when box size and shape are fixed, or both.

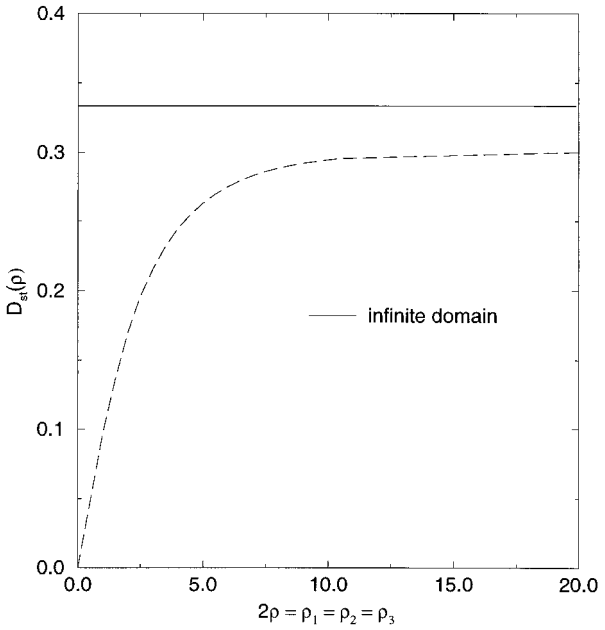

Figure 4. Steady state component of normalized $\kappa_1^{[2]}$, D_{st}, versus dimensionless box size $2\rho = \rho_1 = \rho_2 = \rho_3$. Horizontal line represents asymptote for $2\rho \to \infty$.

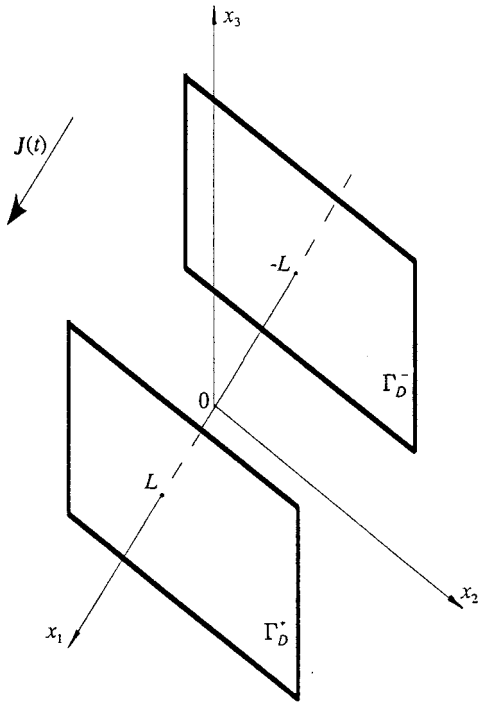

Figure 5. Flow domain Ω between infinite planar Dirichlet boundaries.

2.2. Uniform Flow Between Infinite Dirichlet Boundaries

To complement expressions for effective hydraulic conductivity previously developed for steady state flow by *Paleologos et al.* [1996], we consider the special case where the lateral mean no-flow boundaries are far relative to λ_1 so that $\rho_2 = L_2/\lambda_1$ and $\rho_3 = L_3/\lambda_1$ are very large and mathematically infinite. To be consistent with *Paleologos et al.* [1996], we place the origin of the Cartesian coordinates midway between the Dirichlet planes so that they are spaced a distance $2L$ apart along the x_1 axis (Figure 5).

Like *Paleologos et al.* [1996], we evaluate $\kappa_1^{[2]}(\mathbf{x}, t_D)$ midway between the Dirichlet plates at $\mathbf{x} = 0$. For this point, D_{st} in (29) is given by (B1) and $b(t_D)$ by either (B2) or (B3), where $2\rho = 2L/\lambda_1$. We show in Appendix C[1] that (B1) is the compact sum of infinite series solutions given by (19) or (21) of *Paleologos et al.* [1996]. For statistically isotropic media, D_{st} is given by (B6) and $b(t_D)$ is given by either (B7) or (B8).

When $\rho \to \infty$, (B1) and (B2) reduce to (B13). In the special anisotropic case where $\varepsilon_2 = \varepsilon_3 = \varepsilon$, the steady state part of (B12) can be integrated (Appendix D) to obtain

$$D_{st} = \frac{\varepsilon^2}{(1-\varepsilon^2)^{3/2}}\left[\frac{1}{2}\ln\frac{1+\sqrt{1-\varepsilon^2}}{1-\sqrt{1-\varepsilon^2}} - \sqrt{1-\varepsilon^2}\right] \quad 0 \le \varepsilon \le 1$$

$$D_{st} = 1/3 \qquad \varepsilon = 1 \tag{30}$$

$$D_{st} = \frac{\varepsilon^2}{(1-\varepsilon^2)^{3/2}}\left[-\frac{\pi}{2} + \text{arcctn}\ \sqrt{\varepsilon^2-1} + \sqrt{\varepsilon^2-1}\right] \quad \varepsilon \ge 1.$$

From expansions of $\ln x$ and arcctn x [*Dwight*, 1961, equation 601.2, p. 137, equation 506.1, p. 119] it follows that this new

[1]Appendixes C–E are available with entire article on microfiche. Order by mail from American Geophysical Union, 2000 Florida Avenue, N. W., Washington, DC 20009 or by phone at 800-966-2481; $2.50. Document W97-002. Payment must accompany order.

expression for $D_{st}(\varepsilon)$ is continuous at $\varepsilon = 1$, where it reduces to the well-established isotropic value of 1/3. For statistically isotropic media, (29) and (B13) reduce to (45) of *Dagan* [1982].

Since (B1) was developed under the condition $\rho > 0$, it cannot be used to derive the formal limit of $\kappa_1^{[2]}$ as $\rho \to 0$. However, (B1) derives from (C23),

$$\frac{\kappa_1^{[2]}(t_D)}{\sigma_Y^2 K_G} = \pi \sum_{n=1}^{\infty} n^2 \int_{-\infty}^{+\infty}\int_{-\infty}^{+\infty} \frac{1 - e^{-(\pi^2 n^2/\rho^2 + (k_2^*/\varepsilon_2)^2 + (k_3^*/\varepsilon_3)^2)t_D}}{\pi^2 n^2 + [(k_2^*/\varepsilon_2)^2 + (k_3^*/\varepsilon_3)^2]\rho^2} \cdot \left[(-1)^{n+1} e^{-\rho\sqrt{1+k^{*2}}} \left(\frac{1}{\sqrt{1+k^{*2}}} + \frac{2\rho}{(1+k^{*2})\rho^2 + \pi^2 n^2} \right) + \frac{2\rho}{(1+k^{*2})\rho^2 + \pi^2 n^2} \right] \frac{\rho^2\, dk_2^*\, dk_3^*}{(1+k^{*2})\rho^2 + \pi^2 n^2}. \quad (31)$$

where $k^{*2} = k_2^{*2} + k_3^{*2}$. It was shown by *Paleologos et al.* [1996] that the steady state part of (31) tends to zero as $\rho \to 0$. The same is true for the transient part (Appendix D).

The limit $\varepsilon_2 = \varepsilon_3 = \varepsilon \to 0$ corresponds to mean flow parallel to channels with mutually uncorrelated hydraulic conductivities. Then $\lim_{\varepsilon \to 0} \kappa_1^{[2]}(t_D) = 0$ and $K_{eff,1}$ reduces to the arithmetic mean, K_A. The limit $\varepsilon_2 = \varepsilon_3 = \varepsilon \to \infty$ corresponds to mean flow perpendicular to a stratified formation. Then $\lim_{\varepsilon \to \infty} D_{st} = 1$, and $K_{eff,1}$ reduces to the harmonic mean, K_H. The limit of $b(t_D)$ as $\varepsilon \to \infty$ varies between the bounds $\lim_{\varepsilon \to \infty} b(t_D = 0) = 1$ and $\lim_{\varepsilon \to \infty} b(t_D \to \infty) = 0$.

Figure 6a shows how the steady state component of $\kappa_1^{[2]}(t_D)$, D_{st}, in (B6) varies with the dimensionless distance 2ρ between mean Dirichlet boundaries. It can be seen that at $2\rho \geq 7$, D_{st} is virtually equal to its asymptotic value of 1/3 corresponding to an infinite domain. Thus a separation distance of about seven integral scales between the Dirichlet boundaries is enough to consider the medium as being unbounded for the purpose of assigning to it an effective hydraulic conductivity. Our Figure 6a differs slightly from Figure 2 of *Paleologos et al.* [1996], particularly in that our D_{st} reaches the asymptote faster. While in their figure D_{st} reaches 96% of its asymptotic value of 1/3 at $2\rho = 20$, in our figure it reaches it at $2\rho = 4.4$. As our expression for D_{st} is obtained by analytical summation of the infinite series used by *Paleologos et al.* [1996] to express D_{st}, it is less prone to numerical error and we therefore expect our computational results to be somewhat more accurate. Our semilog plot of the same curve in Figure 6b shows that D_{st} approaches its asymptote at a near-exponential rate. Figure 7 shows how $b(t_D)$ in (B8) varies with dimensionless time when $2\rho = 1$, 3, and ∞. It can be seen that at a separation distance of about three integral scales, the effect of Dirichlet boundaries on the transient behavior of effective hydraulic conductivity, midway between these boundaries, is practically zero.

Figures 8 and 9 demonstrate the influence of anisotropy ratio $\varepsilon_2 = \varepsilon_3 = \varepsilon$ on the steady state and transient components of $\kappa_1^{[2]}(t_D)$ in (30) and (B13), respectively. Figure 8 depicts the manner in which D_{st} increases with ε from 0 to its theoretical asymptotic value of 1. Figure 9 demonstrates that both the contribution of $b(t)$ to $\kappa_1^{[2]}(t_D)$, and the relaxation time t_r, increase with the anisotropy ratio ε.

3. Arbitrary Time Variation

When the uniform mean hydraulic gradient $J_1(t)$ varies arbitrarily with time, the mean flux is given by the time-nonlocal expression (19). The kernel $\kappa^{*[2]}(\mathbf{x}, t_D)$ of the corresponding time-convolution integral can be obtained either directly from (20) or indirectly via [*Tartakovsky and Neuman*, this issue (b), (75)]

$$\kappa_1^{*[2]}(\mathbf{x}, t_D) = -\frac{\partial K_{eff,1}^{[2]}(\mathbf{x}, t_D)}{\partial t_D} = \frac{\partial \kappa_1^{[2]}(\mathbf{x}, t_D)}{\partial t_D} = -\sigma_Y^2 K_G \frac{\partial b(\mathbf{x}, t_D)}{\partial t_D}. \quad (32)$$

Applying (31) to (A1) or (A2) yields $\kappa_1^{*[2]}(\mathbf{x}, t_D)$ for our box in the form of (A5) or (A6), respectively. Evaluating (A6) numerically at $\chi_1 = 0.1$, 0.2, 0.3, 0.5, far from mean no-flow boundaries, shows that $\kappa_1^{*[2]}$ varies with distance from the mean Dirichlet boundaries (Figure 10). A comparison of Figures 10 and 2 demonstrates that this spatial variation is less pronounced for $\kappa_1^{*[2]}$ than for $\kappa_1^{[2]}$. Below we evaluate the former at the midpoint of each flow domain.

In the box the midpoint lies at $\chi = 0.5$. The corresponding time behaviors of $\kappa_1^{*[2]}(t_D)$ (normalized by $\sigma_Y^2 K_G$) at different values of $2\rho = \rho_1 = \rho_2 = \rho_3$ are illustrated in Figure 11. A comparison of Figures 11 and 3 demonstrates that $\kappa_1^{*[2]}(t_D)$ is less sensitive to 2ρ than is $\kappa_1^{[2]}(t_D)$. If the domain is bounded by two infinite Dirichlet planes, its midpoint is placed at $\mathbf{x} = 0$. Figure 12 shows how normalized $\kappa_1^{*[2]}(t_D)$ varies with t_D in statistically isotropic media for dimensionless distances $2\rho = 1$, 3, ∞ when $b(t_D)$ is given by (B8). Figure 13 illustrates the same for infinite statistically anisotropic media with $b(t_D)$ given by (B12). Comparisons of Figure 12 with Figure 7 and of Figure 13 with Figure 9 demonstrate that the kernel $\kappa_1^{*[2]}(t_D)$ is less sensitive to location between Dirichlet boundaries, and to statistical anisotropy, than is $\kappa_1^{[2]}(t_D)$.

Tartakovsky and Neuman [this issue (b)] found previously that in an infinite three-dimensional statistically isotropic domain, the effect of temporal nonlocality is small for $\sigma_Y^2 \leq 1$ when the mean hydraulic gradient is spatially uniform. Figures 11 and 12 suggest that the same is true for anisotropic bounded domains.

4. Conclusions

Our analysis leads to the following conclusions:

1. On the basis of the nonlocal formalism of transient flow in randomly heterogeneous media developed by *Tartakovsky and Neuman* [this issue (a)], we derived first-order analytical expressions for effective hydraulic conductivity under three-dimensional transient flow through a boxed-shaped domain due to a mean hydraulic gradient that varies slowly in space and time. When the mean gradient varies rapidly in time, the Laplace transform of the mean flux is local but its real-time equivalent includes a temporal convolution integral; we developed analytical expressions for the real-time kernel of this convolution integral. The box is embedded within a statistically homogeneous natural log hydraulic conductivity field $Y = \ln K$ that is Gaussian and exhibits an anisotropic exponential spatial correlation structure.

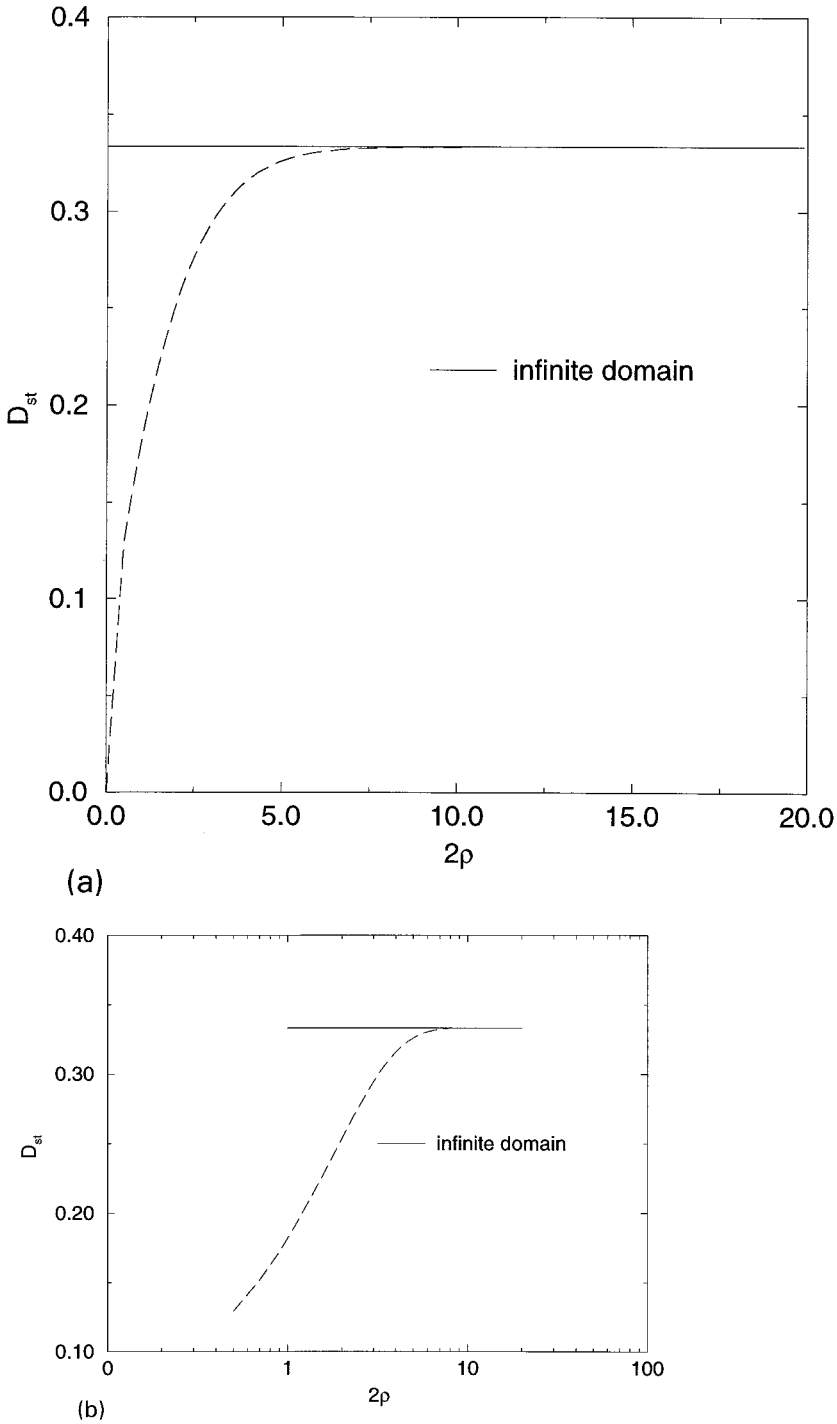

Figure 6. (a) Arithmetic and (b) semilogarithmic plots of steady state component of normalized $\kappa_1^{[2]}$, D_{st}, versus dimensionless distance 2ρ between infinite Dirichlet boundaries in isotropic domain. Horizontal line represents asymptote for $2\rho \to \infty$.

2. Under transient flow, both the effective hydraulic conductivity and the time-convolution kernel vary with distance from the mean prescribed head boundaries, the first to a greater extent than the second. Although mass balance requires that this effect vanish asymptotically as flow approaches steady state, it nevertheless persists for a considerable time.

3. Both the residual component of the effective hydraulic conductivity and the time-convolution kernel diminish as the ratio between box dimensions and integral scales of Y becomes small. The relaxation time required for transient effects to dissipate increases with this ratio, as does the residual component of the of the steady state effective hydraulic conductivity of a box.

4. Our results generalize, and simplify, expressions obtained previously by *Paleologos et al.* [1996] for the steady state effective hydraulic conductivity of a domain bounded by two mean constant head Dirichlet boundaries of infinite extent. We also developed a simple new expression for the steady state

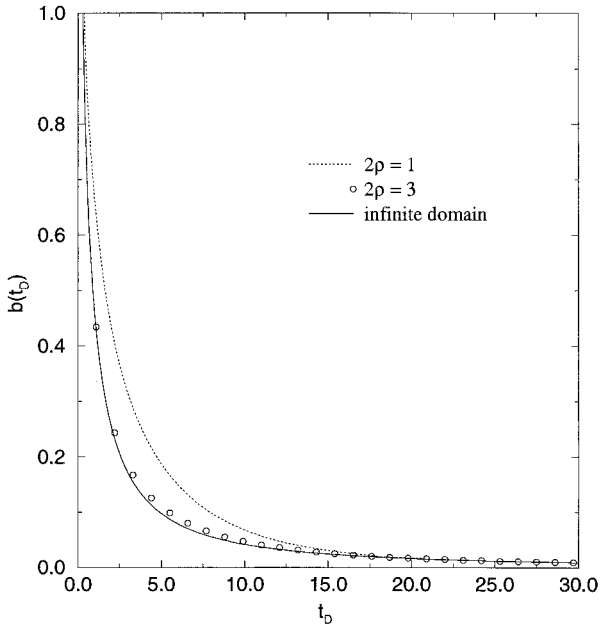

Figure 7. Transient component of normalized $\kappa_1^{[2]}$, $b(t_D)$, versus dimensionless time t_D for various dimensionless distances 2ρ between infinite Dirichlet boundaries in isotropic domain.

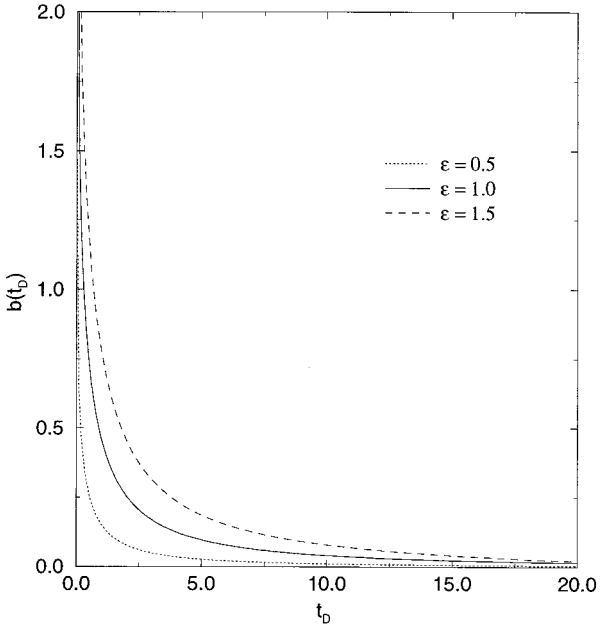

Figure 9. Transient component of normalized $\kappa_1^{[2]}$, $b(t_D)$, in infinite domain versus dimensionless time t_D for various anisotropy ratios ε.

effective hydraulic conductivity of an infinite domain that is isotropic in the plane of any two principal Cartesian coordinates when mean flow takes place parallel to one of them. Limiting cases include mean flow parallel to channels with mutually uncorrelated hydraulic conductivities and mean flow perpendicular to random strata.

5. In the case of steady state flow between two parallel mean Dirichlet boundaries, a separation distance of about seven integral scales between them is enough to consider the distance infinite when the lateral mean no-flow boundaries are separated by equal or larger distances. The corresponding effective conductivity approaches its infinite-domain asymptote at a near-exponential rate with separation distance between the mean Dirichlet boundaries.

6. Our expressions for effective hydraulic conductivity are nominally limited to mildly heterogeneous media with log conductivity variance $\sigma_Y^2 < 1$. *Paleologos et al.* [1996] employed the *Landau and Lifshitz* [1960] conjecture to extend their steady state effective conductivity expressions into the domain of strongly heterogeneous media with $\sigma_Y^2 \geq 1$, and the same could be

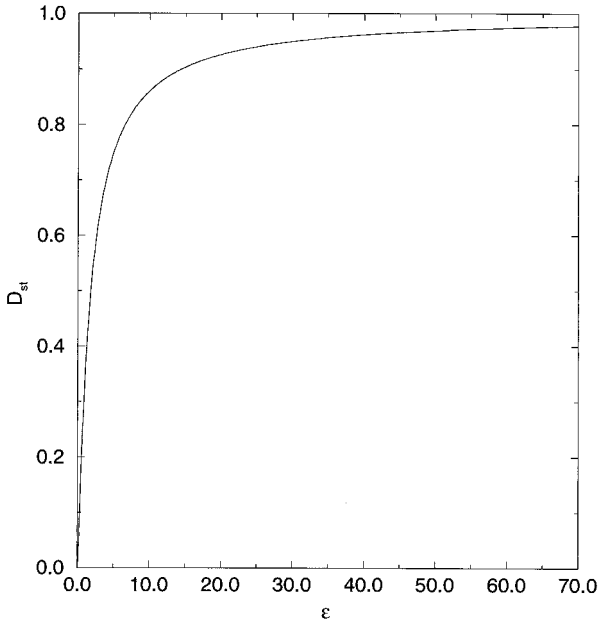

Figure 8. Steady state component of normalized $\kappa_1^{[2]}$, D_{st}, in infinite domain versus anisotropy ratio ε.

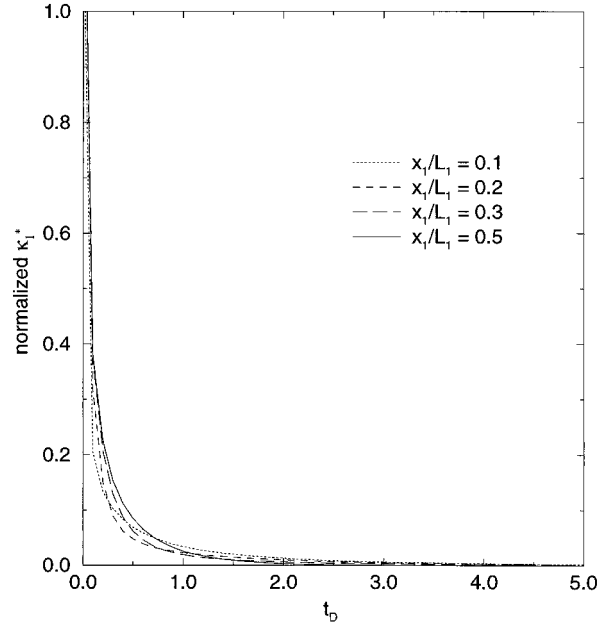

Figure 10. Spatial variation of normalized kernel $\kappa_1^{*[2]}$ in box with $\rho_1 = 5$ and $\rho_2 = \rho_3 = 100$.

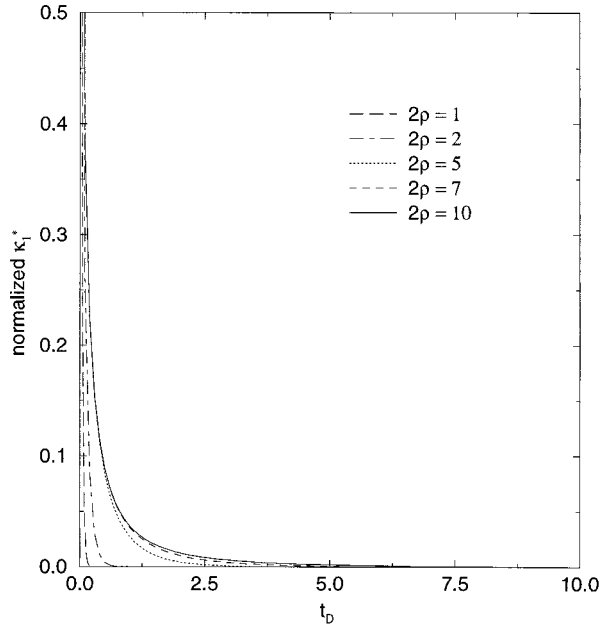

Figure 11. Normalized kernel $\kappa_1^{*[2]}$ versus dimensionless time t_D for various dimensionless box sizes $2\rho = \rho_1 = \rho_2 = \rho_3$.

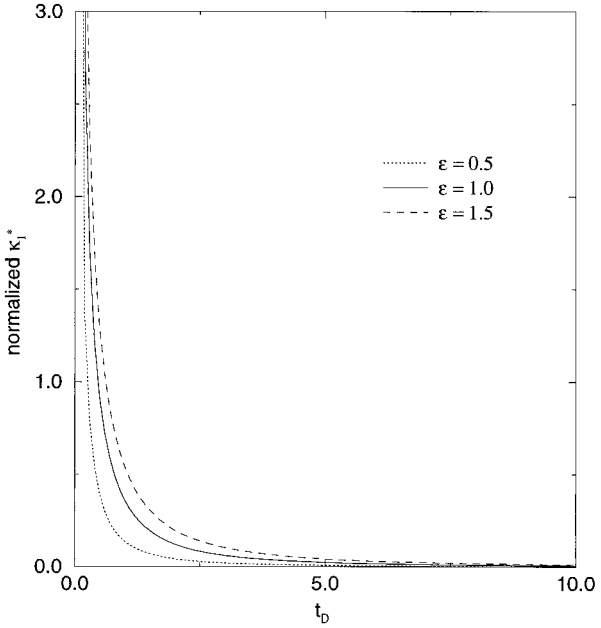

Figure 13. Normalized kernel $\kappa_1^{*[2]}$ in infinite domain versus dimensionless time t_D for various anisotropy ratios ε.

done with our expressions. The circumstances under which this might be valid for transient expressions remain unexplored.

7. *Tartakovsky and Neuman* [this issue (b)] found previously that in an infinite statistically isotropic domain with mild heterogeneity, the effect of temporal nonlocality is small when the mean hydraulic gradient is spatially uniform. We found the same to be true for anisotropic bounded domains.

8. The effective hydraulic conductivity we speak of represents ensemble averages (expectations) of values one would obtain by performing measurements on porous blocks selected at random from a statistically homogeneous medium and subjected to a spatially uniform hydraulic gradient that varies slowly in time. When the block size is very small, the average of measured hydraulic conductivities is their arithmetic mean, and the variance of their natural logarithms is σ_Y^2, the variance of Y. As block size increases, the mean of the measurements diminishes towards a nonzero asymptote while their variance reduces asymptotically to zero. The same holds true in Laplace space when the mean hydraulic gradient varies rapidly in time but not in space.

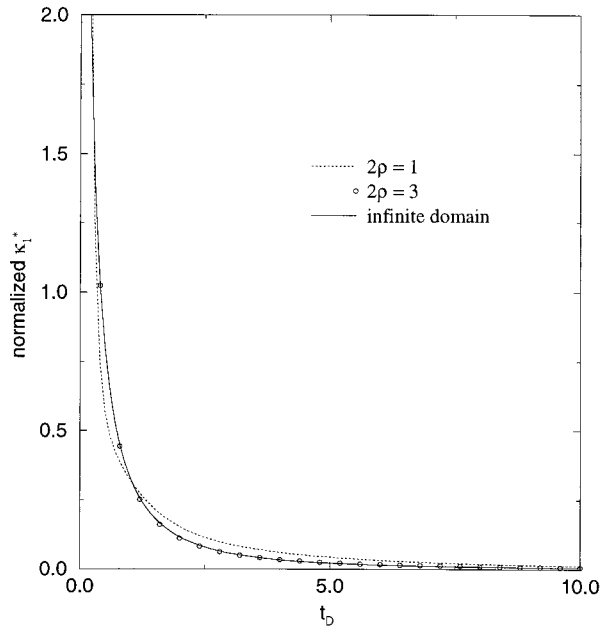

Figure 12. Normalized kernel $\kappa_1^{*[2]}$ versus dimensionless time t_D for various dimensionless distances 2ρ between infinite Dirichlet boundaries in isotropic domain.

Appendix A

Substituting (28) and (27), written in terms of normalized coordinates $\mathbf{x}$ and box dimensions $l_i = L_i/\lambda_i$, $(i = 1, 2, 3)$, into (22) and (24), then introducing the dimensionless variables $\chi_i = x_i/l_i$, $\zeta_i = y_i/l_i$, $\rho_i = \varepsilon_i l_i$, $\varepsilon_i = \lambda_i/\lambda_1$, $t_D = K_G t/S\lambda_1^2$ leads to the following expression for $\kappa_1^{[2]}$,

$$\frac{\kappa_1^{[2]}(\chi, t_D)}{\sigma_Y^2 K_G} = \frac{2\pi^2}{\rho_1^2}\int_0^{t_D}\int_0^1\int_0^1\int_0^1 \exp\left[-((\chi_1-\zeta_1)^2\rho_1^2 + (\chi_2-\zeta_2)^2\rho_2^2 + (\chi_3-\zeta_3)^2\rho_3^2)^{1/2}\right] \sum_{m=1}^{\infty} m^2 e^{-\pi^2\eta_D m^2/\rho_1^2}\cos\pi m\chi_1\cos\pi m\zeta_1 \cdot\left[1 + 2\sum_{n=1}^{\infty} e^{-\pi^2\eta_D n^2/\rho_2^2}\cos\pi n\chi_2\cos\pi n\zeta_2\right] \cdot\left[1 + 2\sum_{j=1}^{\infty} e^{-\pi^2\eta_D j^2/\rho_3^2}\cos\pi j\chi_3\cos\pi j\zeta_3\right] d\zeta_3\, d\zeta_2\, d\zeta_1\, d\tau_D. \quad \text{(A1)}$$

Using the method of images (Appendix E) yields, with the aid of Poisson's summation formula [*Stakgold*, 1979, equation (3.28), p. 140], an alternative expression for $\kappa_1^{[2]}$:

$$\frac{\kappa_1^{[2]}(\chi, t_D)}{\sigma_Y^2 K_G} = \frac{\rho_1\rho_2\rho_3}{8\pi^{3/2}} \int_0^{t_D}\int_0^1\int_0^1\int_0^1 \eta_D^{-5/2} \exp\left[-((\chi_1-\zeta_1)^2\rho_1^2 + (\chi_2-\zeta_2)^2\rho_2^2 + (\chi_3-\zeta_3)^2\rho_3^2)^{1/2}\right]$$
$$\cdot \sum_{m=-\infty}^{\infty} \left\{ \left[\frac{1}{2} - \frac{\rho_1^2(\chi_1+\zeta_1+2m)^2}{4\eta_D}\right] \cdot \exp\left[-(\chi_1+\zeta_1+2m)^2\rho_1^2/4\eta_D\right] + \left[\frac{1}{2} - \frac{\rho_1^2(\chi_1-\zeta_1+2m)^2}{4\eta_D}\right] \cdot \exp\left[-(\chi_1-\zeta_1+2m)^2\rho^2/4\eta_D\right] \right\}$$
$$\cdot \sum_{n=-\infty}^{\infty} \{\exp\left[-\rho_2^2(\chi_2+\zeta_2+2n)^2/4\eta_D\right] + \exp\left[-\rho_2^2(\chi_2-\zeta_2+2n)^2/4\eta_D\right]\}$$
$$\cdot \sum_{j=-\infty}^{\infty} \{\exp\left[-\rho_3^2(\chi_3+\zeta_3+2j)^2/4\eta_D\right] + \exp\left[-\rho_3^2(\chi_3-\zeta_3+2j)^2/4\eta_D\right]\}\, d\zeta_3\, d\zeta_2\, d\zeta_1\, d\eta_D. \quad \text{(A2)}$$

Evaluating the time integral in (A2) yields $\kappa_1^{[2]}(\chi, t_D) = \sigma_Y^2 K_G[D_{st}(\chi) - b(\chi, t_D)]$ where

$$D_{st}(\chi) = 2\int_0^1\int_0^1\int_0^1 \exp\left[-((\chi_1-\zeta_1)^2\rho_1^2 + (\chi_2-\zeta_2)^2\rho_2^2 + (\chi_3-\zeta_3)^2\rho_3^2)^{1/2}\right]$$
$$\cdot \sum_{m=1}^{\infty} \cos\pi m\chi_1 \cos\pi m\zeta_1\, d\zeta_3\, d\zeta_2\, d\zeta_1 + \frac{4}{\rho_1^2}\int_0^1\int_0^1\int_0^1$$
$$\cdot \exp\left[-((\chi_1-\zeta_1)^2\rho_1^2 + (\chi_2-\zeta_2)^2\rho_2^2 + (\chi_3-\zeta_3)^2\rho_3^2)^{1/2}\right]$$
$$\cdot \sum_{n=1}^{\infty}\sum_{m=1}^{\infty} m^2 \frac{\cos\pi m\chi_1 \cos\pi m\zeta_1 \cos\pi n\chi_2 \cos\pi n\zeta_2}{m^2/\rho_1^2 + n^2/\rho_2^2}$$
$$\cdot d\zeta_3\, d\zeta_2\, d\zeta_1 + \frac{4}{\rho_1^2}\int_0^1\int_0^1\int_0^1 \exp\left[-((\chi_1-\zeta_1)^2\rho_1^2 + (\chi_2-\zeta_2)^2\rho_2^2 + [\chi_3-\zeta_3)^2\rho_3^2)^{-1/2}\right] \sum_{j=1}^{\infty}\sum_{m=1}^{\infty} m^2$$
$$\cdot \frac{\cos\pi j\chi_3 \cos\pi j\zeta_3 \cos\pi m\chi_1 \cos\pi m\zeta_1}{m^2/\rho_1^2 + j^2/\rho_3^2}\, d\zeta_3 d\zeta_2 d\zeta_1$$
$$+ \frac{8}{\rho_1^2}\int_0^1\int_0^1\int_0^1 \exp\left[-((\chi_1-\zeta_1)^2\rho_1^2 + (\chi_2-\zeta_2)^2\rho_2^2 + (\chi_3-\zeta_3)^2\rho_3^2)^{1/2}\right] \sum_{l=1}^{\infty}\sum_{n=1}^{\infty}\sum_{m=1}^{\infty} m^2$$
$$\cdot \frac{\cos\pi m\chi_1 \cos\pi m\zeta_1 \cos\pi n\chi_2 \cos\pi n\zeta_2 \cos\pi l\chi_3 \cos\pi l\zeta_3}{m^2/\rho_1^2 + n^2/\rho_2^2 + l^2/\rho_3^2}$$
$$\cdot d\zeta_3 d\zeta_2 d\zeta_1 \quad \text{(A3)}$$

and

$$b(\chi, t_D) = 2\int_0^1\int_0^1\int_0^1 \exp\left[-((\chi_1-\zeta_1)^2\rho_1^2 + (\chi_2-\zeta_2)^2\rho_2^2 + (\chi_3-\zeta_3)^2\rho_3^2)^{1/2}\right] \sum_{m=1}^{\infty} e^{-\pi^2 m^2 t_D/\rho_1^2} \cos\pi m\chi_1 \cos\pi m\zeta_1\, d\zeta_3\, d\zeta_2\, d\zeta_1$$
$$+ \frac{4}{\rho_1^2}\int_0^1\int_0^1\int_0^1 \exp\left[-((\chi_1-\zeta_1)^2\rho_1^2 + (\chi_2-\zeta_2)^2\rho_2^2 + (\chi_3-\zeta_3)^2\rho_3^2)^{1/2}\right] \sum_{n=1}^{\infty}\sum_{m=1}^{\infty} m^2 \frac{e^{-\pi^2(m^2/\rho_1^2+n^2/\rho_2^2)t_D}}{m^2/\rho_1^2+n^2/\rho_2^2}$$
$$\cdot \cos\pi m\chi_1 \cos\pi m\zeta_1 \cos\pi n\chi_2 \cos\pi n\zeta_2\, d\zeta_3\, d\zeta_2\, d\zeta_1$$
$$+ \frac{4}{\rho_1^2}\int_0^1\int_0^1\int_0^1 \exp\left[-((\chi_1-\zeta_1)^2\rho_1^2 + (\chi_2-\zeta_2)^2\rho_3^2 + (\chi_3-\zeta_3)^2\rho_3^2)^{1/2}\right] \sum_{j=1}^{\infty}\sum_{m=1}^{\infty} m^2 \frac{e^{-\pi^2(m^2/\rho_1^2+j^2/\rho_3^2)t_D}}{m^2/\rho_1^2+j^2/\rho_3^2}$$
$$\cdot \cos\pi m\chi_1 \cos\pi m\zeta_1 \cos\pi j\chi_3 \cos\pi j\zeta_3\, d\zeta_3\, d\zeta_2\, d\zeta_1$$
$$+ \frac{8}{\rho_1^2}\int_0^1\int_0^1\int_0^1 \exp\left[-((\chi_1-\zeta_1)^2\rho_1^2 + (\chi_2-\zeta_2)^2\rho_2^2 + (\chi_3-\zeta_3)^2\rho_3^2)^{1/2}\right] \sum_{j=1}^{\infty}\sum_{n=1}^{\infty}\sum_{m=1}^{\infty} m^2 \frac{e^{-\pi^2(m^2/\rho_1^2+n^2/\rho_2^2+j^2/\rho_3^2)t_D}}{m^2/\rho_1^2+n^2/\rho_2^2+j^2/\rho_2^2} \cos\pi m\chi_1$$
$$\cdot \cos\pi m\zeta_1 \cdot \cos\pi n\chi_2 \cos\pi n\zeta_2 \cos\pi j\chi_3$$
$$\cdot \cos\pi j\zeta_3\, d\zeta_3\, d\zeta_2\, d\zeta_1. \quad \text{(A4)}$$

Taking the time derivative of (A1) and (A2) yields, respectively,

$$\frac{\kappa_1^{*[2]}(\chi, t_D)}{\sigma_Y^2 K_G} = \frac{2\pi^2}{\rho_1^2}\int_0^1\int_0^1\int_0^1 \exp\left[-((\chi_1-\zeta_1)^2\rho_1^2 + (\chi_2-\zeta_2)^2\rho_2^2 + (\chi_3-\zeta_3)^2\rho_3^2)^{1/2}\right]$$
$$\cdot \sum_{m=1}^{\infty} m^2 e^{-\pi^2 t_D m^2/\rho_1^2} \cos\pi m\chi_1 \cos\pi m\zeta_1 \cdot \left[1 + 2\sum_{n=1}^{\infty} e^{-\pi^2 t_D n^2/\rho_2^2} \cos\pi n\chi_2 \cos\pi n\zeta_2\right]$$
$$\cdot \left[1 + 2\sum_{j=1}^{\infty} e^{-\pi^2 t_D j^2/\rho_3^2} \cos\pi j\chi_3 \cos\pi j\zeta_3\right] d\zeta_3\, d\zeta_2\, d\zeta_1 \quad \text{(A5)}$$

and

$$\frac{\kappa_1^{*[2]}(\chi, t_D)}{\sigma_Y^2 K_G} = \frac{\rho_1\rho_2\rho_3}{8\pi^{3/2}} \int_0^1\int_0^1\int_0^1 t_D^{-5/2} \exp\left[-((\chi_1-\zeta_1)^2\rho_1^2 + (\chi_2-\zeta_2)^2\rho_2^2 + (\chi_3-\zeta_3)^2\rho_3^2)^{1/2}\right] \cdot \sum_{m=-\infty}^{\infty} \left\{ \left[\frac{1}{2} - \frac{\rho_1^2(\chi_1+\zeta_1+2m)^2}{4t_D}\right] \cdot \exp\left[-(\chi_1+\zeta_1+2m)^2\rho_1^2/4t_D\right] + \left[\frac{1}{2} - \frac{\rho_1^2(\chi_1-\zeta_1+2m)^2}{4t_D}\right] \cdot \exp\left[-(\chi_1-\zeta_1+2m)^2\rho^2/4\eta_D\right]\right\} \cdot \sum_{n=-\infty}^{\infty} \{\exp\left[-\rho_2^2(\chi_2+\zeta_2+2n)^2/4t_D\right] + \exp\left[-\rho_2^2(\chi_2-\zeta_2+2n)^2/4t_D\right]\} \cdot \sum_{j=-\infty}^{\infty} \{\exp\left[-\rho_3^2(\chi_3+\zeta_3+2j)^2/4t_D\right] + \exp\left[-\rho_3^2(\chi_3-\zeta_3+2j)^2/4t_D\right]\} \, d\zeta_3\, d\zeta_2\, d\zeta_1. \tag{A6}$$

Appendix B

The steady state and transient components of $\kappa_1^{[2]}(\mathbf{0}, t_D)$ are derived in Appendix C. From (C49) and (C26) it follows that

$$D_{st} = \frac{1}{2\pi}\int_{k^*=0}^{\infty}\int_{\theta=0}^{2\pi} k^*\left\{\frac{1}{B(A+B)^2} + \frac{A^2+B^2}{B(A^2-B^2)^2}\frac{2}{e^{2\rho B}-1} - \frac{2A}{(A^2-B^2)^2}\frac{2}{e^{2\rho A}-1} - \frac{e^{-\rho B}}{(A^2-B^2)^2} \cdot \left[\frac{A^2+B^2}{B} - 2\rho(A^2-B^2)\right] \sinh^{-1}(\rho B) + \frac{A[2B-\rho(A^2-B^2)]e^{-\rho B}}{B(A^2-B^2)^2}\sinh^{-1}(\rho A) + \frac{\rho}{A^2-B^2}\left[e^{-2\rho B}-1\right]\sinh^{-2}(\rho B)\right\} d\theta\, dk^* \tag{B1}$$

where A and B are defined in (B4) below. By virtue of (C24) and (C25),

$$b(t_D) = \pi\sum_{n=1}^{\infty}\int_{k^*=0}^{+\infty}\int_{\theta=0}^{2\pi} k^* e^{-A^2 t_D}\,\phi_2(n, k^*, \theta, t_D)\, d\theta\, dk^* \tag{B2}$$

$$\phi_2 = \frac{n^2\rho^2 e^{-\pi^2 n^2\rho^{-2}t_D}}{(\pi^2n^2+\rho^2A^2)(\pi^2n^2+\rho^2B^2)} \cdot \left[\frac{2\rho}{\pi^2n^2+\rho^2B^2} + (-1)^{n+1}e^{-\rho B}\left(\frac{1}{B} + \frac{2\rho}{\pi^2n^2+\rho^2B^2}\right)\right].$$

Analogously, by virtue of (C67) and (C63) with $\xi = k^{*2}$, recalling from (C23) that $k'^2\lambda_1^2 = A^2$,

$$b(t_D) = \pi\int_{k^*=0}^{\infty}\int_{\theta=0}^{2\pi} k^* e^{-A^2 t_D} p(k^*, \theta, t_D)\, d\theta\, dk^*,$$

$$2p(\xi, \theta, t_D) = \nu_1\sum_{m=-\infty}^{\infty} e^{2|m|\sqrt{d}}\operatorname{erfc}\beta_1(2m) + \nu_1\sum_{m=-\infty}^{\infty} e^{-2|m|\sqrt{d}}\operatorname{erfc}\beta_2(2m) + \nu_2\sum_{m=-\infty}^{\infty}|m|\, e^{2|m|\sqrt{d}}\operatorname{erfc}\beta_1(2m) - \nu_2\sum_{m=-\infty}^{\infty}|m| \cdot e^{-2|m|\sqrt{d}}\operatorname{erfc}\beta_2(2m) - \nu_3\sum_{m=-\infty}^{\infty} e^{2|m|\sqrt{d}}\, e^{-\beta_1^2(2m)} - \nu_3\sum_{m=-\infty}^{\infty} e^{-2|m|\sqrt{d}}\, e^{-\beta_2^2(2m)} + \nu_4\sum_{m=-\infty}^{\infty} e^{2|m|\sqrt{a}}\operatorname{erfc}\gamma_1(2m) + \nu_4\sum_{m=-\infty}^{\infty} e^{-2|m|\sqrt{a}}\operatorname{erfc}\gamma_2(2m) - \nu_5\sum_{m=-\infty}^{\infty} e^{|2m+1|\sqrt{d}} \cdot \operatorname{erfc}\beta_1(2m+1) - \nu_5\sum_{m=-\infty}^{\infty} e^{-|2m+1|\sqrt{d}}\operatorname{erfc}\beta_2(2m+1) - \nu_6\sum_{m=-\infty}^{\infty}|2m+1|\, e^{|2m+1|\sqrt{d}}\operatorname{erfc}\beta_1(2m+1) + \nu_6\sum_{m=-\infty}^{\infty}|2m+1|\, e^{-|2m+1|\sqrt{d}}\operatorname{erfc}\beta_2(2m+1) + \nu_7\sum_{m=-\infty}^{\infty} e^{|2m+1|\sqrt{d}}\, e^{-\beta_1^2(2m+1)} + \nu_7\sum_{m=-\infty}^{\infty} e^{-|2m+1|\sqrt{d}}\, e^{-\beta_2^2(2m+1)} - \nu_8\sum_{m=-\infty}^{\infty} e^{|2m+1|\sqrt{a}}\operatorname{erfc}\gamma_1(2m+1) - \nu_8\sum_{m=-\infty}^{\infty} e^{-|2m+1|\sqrt{a}}\operatorname{erfc}\gamma_2(2m+1). \tag{B3}$$

The coefficients in (B1)–(B3) are defined in (C26), (C65), and (C66) as

$$a = A^2\rho^2 \qquad d = B^2\rho^2$$

$$A^2 = (k_2^*/\varepsilon_2)^2 + (k_3^*/\varepsilon_3)^2 = k^{*2}R_1^2 \tag{B4}$$

$$R_1^2 = \frac{\sin^2\theta}{\varepsilon_3^2} + \frac{\cos^2\theta}{\varepsilon_2^2} \qquad B^2 = 1 + k^{*2}$$

$$\nu_1 = \frac{e^{t_D(1+k^{*2})}}{2\pi^2\sqrt{1+k^{*2}}}\left\{\frac{2(1+k^{*2})}{(R_1^2k^{*2}-1-k^{*2})^2} + \frac{1+2t_D(1+k^{*2})}{R_1^2k^{*2}-1-k^{*2}}\right\}$$

$$\nu_2 = \frac{\rho e^{t_D(1+k^{*2})}}{\pi^2(R_1^2k^{*2}-1-k^{*2})}$$

$$\nu_3 = \frac{\sqrt{t_D}\, e^{t_D(1+k^{*2})}}{\pi^{5/2}(R_1^2 k^{*2} - 1 - k^{*2})}$$

$$\nu_4 = -\frac{R_1 k^* e^{t_D R_1^2 k^{*2}}}{\pi^2 (R_1^2 k^{*2} - 1 - k^{*2})^2}$$

$$\nu_5 = e^{-\rho\sqrt{1+k^{*2}}}\left\{\nu_1 + \frac{\rho e^{t_D(1+k^{*2})}}{2\pi^2(R_1^2 k^{*2} - 1 - k^{*2})}\right\}$$

$$\nu_6 = \frac{\nu_2}{2} e^{-\rho\sqrt{1+k^{*2}}}, \quad \nu_7 = \nu_3 e^{-\rho\sqrt{1+k^{*2}}} \tag{B5}$$

$$\nu_8 = e^{-\rho\sqrt{1+k^{*2}}}\left\{\nu_4 + \frac{\rho R_1 k^* e^{t_D R_1^2 k^{*2}}}{2\pi^2\sqrt{1+k^{*2}}(R_1^2 k^{*2} - 1 - k^{*2})}\right\}$$

$$\beta_1(m) = \sqrt{t_D(1+k^{*2})} + \frac{\rho|m|}{2\sqrt{t_D}}$$

$$\beta_2(m) = \sqrt{t_D(1+k^{*2})} - \frac{\rho|m|}{2\sqrt{t_D}}$$

$$\gamma_1(m) = \sqrt{t_D} R_1 k^* + \frac{\rho|m|}{2\sqrt{t_D}}$$

$$\gamma_2(m) = \sqrt{t_D} R_1 k^* - \frac{\rho|m|}{2\sqrt{t_D}}.$$

Expression (B2) is based on an eigenfunction expansion of the Green's function, expression (B3) on the method of images.

For statistically isotropic media $\varepsilon_2 = \varepsilon_3 = 1$, $R_1 = 1$, and the order of integration in (B1)–(B3) is reduced by one,

$$D_{st} = \frac{1}{3} + \frac{1}{2}\int_0^\infty \left\{\frac{2\xi+1}{\sqrt{1+\xi}}\frac{2}{e^{2\rho\sqrt{1+\xi}}-1} - \frac{4\sqrt{\xi}}{e^{2\rho\sqrt{\xi}}-1}\right.$$

$$- e^{-\rho\sqrt{1+\xi}}\left[\frac{2\xi+1}{\sqrt{1+\xi}} + 2\rho\right]\sinh^{-1}(\rho\sqrt{1+\xi})$$

$$+ \sqrt{\xi}\left[2 + \frac{\rho}{\sqrt{1+\xi}}\right]e^{-\rho\sqrt{1+\xi}}\sinh^{-1}(\rho\sqrt{\xi})$$

$$\left. - \rho[e^{-2\rho\sqrt{1+\xi}} - 1]\sinh^{-2}(\rho\sqrt{1+\xi})\right\} d\xi \tag{B6}$$

where the leading term 1/3 represents the first integral in (B1). Setting $k^{*2} = \xi$ in (B2) and (B3) and then integrating over θ leads to

$$b(t_D) = \pi^2 \sum_{n=1}^\infty \int_{\xi=0}^\infty e^{-\xi t_D}\phi_2(n, \xi, t_D)\, d\xi$$

$$\phi_2 = \frac{n^2\rho^2 e^{-\pi^2 n^2 \rho^{-2} t_D}}{(\pi^2 n^2 + \rho^2\xi)(\pi^2 n^2 + \rho^2[1+\xi])}$$

$$\cdot\left[(-1)^{n+1}e^{-\rho\sqrt{1+\xi}}\left(\frac{1}{\sqrt{1+\xi}} + \frac{2\rho}{\pi^2 n^2 + \rho^2[1+\xi]}\right)\right.$$

$$\left. + \frac{2\rho}{\pi^2 n^2 + \rho^2[1+\xi]}\right]. \tag{B7}$$

From (B3),

$$b(t_D) = \frac{1}{3} b_3(t_D) + \int_0^\infty p(\xi, t_D)\, d\xi \tag{B8}$$

where $b_3(t_D)/3$ is the integral with respect to ξ of the first three terms in (C70). According to (D14)–(D28),

$$b_3(t_D) = -2\sqrt{\frac{t_D}{\pi}} + (1+2t_D)e^{t_D}\,\mathrm{erfc}\,\sqrt{t_D}. \tag{B9}$$

The function $p(\xi, t_D)$ represents the remaining terms in (C70),

$$2p(\xi, t_D)$$

$$= \nu_1 \sum_{m=1}^\infty e^{2m\rho\sqrt{1+\xi}}\,\mathrm{erfc}\,[\beta_1(2m)]$$

$$+ \nu_1 \sum_{m=1}^\infty e^{-2m\rho\sqrt{1+\xi}}\,\mathrm{erfc}\,[\beta_2(2m)]$$

$$+ \nu_2 \sum_{m=1}^\infty e^{2m\rho\sqrt{1+\xi}}\,\mathrm{erfc}\,[\beta(2m)]$$

$$- \nu_2 \sum_{m=1}^\infty m e^{-2m\rho\sqrt{1+\xi}}\,\mathrm{erfc}\,[\beta_2(2m)]$$

$$- \nu_3 \sum_{m=1}^\infty e^{2m\rho\sqrt{1+\xi}}\, e^{-\beta_1^2(2m)} - \nu_3 \sum_{m=1}^\infty e^{-2m\rho\sqrt{1+\xi}}\, e^{-\beta_2^2(2m)}$$

$$+ \nu_4 \sum_{m=1}^\infty e^{2m\rho\sqrt{\xi}}\,\mathrm{erfc}\,[\gamma_1(2m)] + \nu_4 \sum_{m=1}^\infty e^{2m\rho\sqrt{\xi}}$$

$$\cdot\,\mathrm{erfc}\,[\gamma_2(2m)] - \nu_5 \sum_{m=0}^\infty e^{(2m+1)\rho\sqrt{1+\xi}}\,\mathrm{erfc}\,[\beta_1(2m+1)]$$

$$- \nu_5 \sum_{m=0}^\infty e^{-(2m+1)\rho\sqrt{1+\xi}}\,\mathrm{erfc}\,[\beta_2(2m+1)]$$

$$- \nu_6 \sum_{m=0}^\infty (2m+1) e^{(2m+1)\rho\sqrt{1+\xi}}\,\mathrm{erfc}\,[\beta_1(2m+1)]$$

$$+ \nu_6 \sum_{m=0}^\infty (2m+1) e^{-(2m+1)\rho\sqrt{1+\xi}}\,\mathrm{erfc}\,[\beta_2(2m+1)]$$

$$+ \nu_7 \sum_{m=0}^\infty e^{(2m+1)\rho\sqrt{1+\xi}}\, e^{-\beta_1^2(2m+1)} + \nu_7 \sum_{m=0}^\infty e^{-(2m+1)\rho\sqrt{1+\xi}}$$

$$\cdot\, e^{-\beta_2^2(2m+1)} - \nu_8 \sum_{m=0}^\infty e^{(2m+1)\rho\sqrt{\xi}}\,\mathrm{erfc}\,[\gamma_1(2m+1)]$$

$$- \nu_8 \sum_{m=0}^\infty e^{-(2m+1)\rho\sqrt{\xi}}\,\mathrm{erfc}\,[\gamma_2(2m+1)] \tag{B10}$$

where, from (C68),

$$\nu_1 = e^{t_D}\left[(1-t_D)\sqrt{1+\xi} - \frac{1}{2\sqrt{1+\xi}}\right]$$

$$\nu_2 = -\rho e^{t_D}$$

$$\nu_3 = -\sqrt{\frac{t_D}{\pi}}\, e^{t_D} \qquad \nu_4 = -\sqrt{\xi}$$

$$\nu_5 = e^{-\rho\sqrt{1+\xi}}\left\{\nu_1 - \frac{\rho}{2}\, e^{t_D}\right\} \tag{B11}$$

$$\nu_6 = \frac{\nu_2}{2}\, e^{-\rho\sqrt{1+\xi}} \qquad \nu_7 = \nu_3 e^{-\rho\sqrt{1+\xi}}$$

$$\nu_8 = e^{-\rho\sqrt{1+\xi}}\left\{\nu_4 - \frac{\rho\sqrt{\xi}}{2\sqrt{1+\xi}}\right\}$$

and from (C69),

$$\beta_1(m) = \sqrt{t_D(1+\xi)} + \frac{\rho|m|}{2\sqrt{t_D}}$$

$$\beta_2(m) = \sqrt{t_D(1+\xi)} - \frac{\rho|m|}{2\sqrt{t_D}}$$

$$\gamma_1(m) = \sqrt{t_D\xi} + \frac{\rho|m|}{2\sqrt{t_D}}$$

$$\gamma_2(m) = \sqrt{t_D\xi} - \frac{\rho|m|}{2\sqrt{t_D}}. \tag{B12}$$

Taking the limit $\rho \to \infty$ in (B1) and (B3) yields

$$\frac{\kappa_1^{[2]}(t_D)}{\sigma_Y^2 K_G} = D_{st} - b(t_D)$$

$$D_{st} = \frac{1}{4\pi}\int_{\xi=0}^{\infty}\int_{\theta=0}^{2\pi} \frac{d\theta\, d\xi}{\sqrt{1+\xi}\left[R_1\sqrt{\xi} + \sqrt{1+\xi}\right]^2} \tag{B13}$$

$$b(t_D) = \frac{\pi}{2}\int_{\xi=0}^{\infty}\int_{\theta=0}^{2\pi} e^{-t_D R_1^2\xi}\left[\nu_1 \operatorname{erfc}\beta - \nu_3 e^{-\beta^2} + \nu_4 \operatorname{erfc}\gamma\right] d\theta\, d\xi,$$

where

$$\nu_1 = \frac{e^{t_D(1+k^{*2})}}{2\pi^2\sqrt{1+k^{*2}}}\left\{\frac{2(1+k^{*2})}{(R_1^2k^{*2} - 1 - k^{*2})^2} + \frac{1 + 2t_D(1+k^{*2})}{R_1^2k^{*2} - 1 - k^{*2}}\right\}$$

$$\nu_3 = \frac{\sqrt{t_D}e^{t_D(1+k^{*2})}}{\pi^{5/2}(R_1^2k^{*2} - 1 - k^{*2})} \tag{B14}$$

$$\nu_4 = -\frac{R_1k^* e^{t_D R_1^2 k^{*2}}}{\pi^2(R_1^2k^{*2} - 1 - k^{*2})^2}$$

$$\beta = \sqrt{(1+k^{*2})t_D} \qquad \gamma = R_1k^*\sqrt{t_D}.$$

Acknowledgment. This work was supported by the U.S. Nuclear Regulatory Commission under contract NRC-04-95-038.

References

Carslaw, H. S., and J. C. Jaeger, *Conduction of Heat in Solids*, 510 pp., Oxford Univ. Press, New York, 1959.

Dagan, G., Analysis of flow through heterogeneous random aquifers, 2, Unsteady flow in confined formations, *Water Resour. Res*., *18*(5), 1571–1585, 1982.

Dwight, H. B., *Tables of Integrals and Other Mathematical Data*, 336 pp., MacMillan, Indianapolis, Ind., 1961.

Erdelyi, A., *Tables of Integral Transforms*, 391 pp., McGraw-Hill, New York, 1954.

Gradshteyn, I. S., and I. M. Ryzhik, *Tables of Integrals, Series, and Products*, 1204 pp., Academic, San Diego, Calif., 1994.

Landau, L. D., and E. M. Lifshitz, *Electrodynamics of Continuous Media*, Pergamon, Tarrytown, N. Y., 1960.

Paleologos, E. K., S. P. Neuman, and D. Tartakovsky, Effective hydraulic conductivity of bounded, strongly heterogeneous porous media, *Water Resour. Res*., *32*(5), 1333–1341, 1996.

Stakgold, I., *Green's Functions and Boundary Value Problems*, 638 pp., John Wiley, New York, 1979.

Tartakovsky, D. M., and S. P. Neuman, Transient flow in bounded randomly heterogeneous domains, 1, Exact conditional moment equations and recursive approximations, *Water Resour. Res*., this issue (a).

Tartakovsky, D. M., and S. P. Neuman, Transient flow in bounded randomly heterogeneous domains, 2, Localization of conditional mean equations and temporal nonlocality effects, *Water Resour. Res*., this issue (b).

S. P. Neuman, Department of Hydrology and Water Resources, The University of Arizona, Building 11, P.O. Box 210011, Tucson, AZ 85721-0011.

D. M. Tartakovsky, Geoanalysis Group, Earth and Environmental Sciences Division, Los Alamos National Laboratory, Los Alamos, NM 87545.

(Received October 4, 1996; revised May 21, 1997; accepted July 10, 1997.)